ELSEVIER

Biophysical Chemistry 125 (2007) 435–443

Biophysical Chemistry

http://www.elsevier.com/locate/biophyschem

Kinetic mechanism of the Zn-dependent aryl-phosphatase activity of *myo*-inositol-1-phosphatase☆

Anna Caselli [a], Mario Casolaro [b], Francesco Ranaldi [a], Giampaolo Manao [a], Guido Camici [a], Eugenio Giachetti [a,*]

[a] *Department of Biochemical Sciences, University of Firenze, Italy*
[b] *Department of Chemical and Biosystem Sciences and Technologies, University of Siena, Italy*

Received 28 July 2006; received in revised form 13 October 2006; accepted 16 October 2006
Available online 20 October 2006

Abstract

Myo-inositol-1-phosphatase (EC 3.1.3.25) is able to hydrolyze *myo*-inositol-1-phosphate in the presence of Mg^{2+} ions at neutral pH, and also *p*-nitrophenyl phosphate in the presence of Zn^{2+}-ions at acidic pH. This enzyme plays a role in phosphatidylinositol cell signalling and is a putative target of lithium therapy in manic depression. We elucidate here the kinetic mechanism of the Zn-dependent activity of *myo*-inositol-1-phosphatase.

As part of this analysis it was necessary to determine the basicity constants of *p*-nitrophenyl phosphate and the stability constant of its metal-complex in the presence of zinc chloride.

We find that the Zn-dependent reaction may be described either by a rapid-equilibrium random mechanism or an ordered steady-state mechanism in which the substrate binds to the free enzyme prior to the metal ion. In both models the Zn-substrate complex acts as a high affinity inhibitor, yielding a dead-end species through its binding to the enzyme-Zn-substrate in rapid-equilibrium or to the enzyme-phosphate complexes in a steady-state model. Phosphate is a competitive inhibitor of the enzyme with respect to the substrate and an uncompetitive inhibitor with respect to zinc ions.

Keywords: *Myo*-inositol-1-phosphatase; Zn-dependent activity; Kinetic mechanism; Aryl-phosphatase activity of *myo*-inositol phosphatase; Zinc:*p*-nitrophenyl-phoshate stability constant

1. Introduction

Zn^{2+}-dependent acid phosphatase activities have been found in various animal tissues [1,2]. We have previously purified the Zn^{2+}-dependent acid phosphatase from bovine brain tissue and characterized its kinetic and molecular properties [3]. This enzyme has powerful Mg^{2+}-dependent *myo*-inositol-1-phosphatase activity and its amino acid sequence is identical to that of the known *myo*-inositol-1-phosphatase (EC 3.1.3.25) from the bovine brain. Thus, the same protein possesses Zn^{2+}-dependent acid *p*-nitrophenyl phosphatase activity and Mg^{2+}-dependent *myo*-inositol-1-phosphatase activity. In the absence of zinc ions, the enzyme does not catalyze the hydrolysis of *p*-nitrophenyl phosphate at pH 5.5. At this pH, Mg^{2+} cannot replace Zn^{2+}. On the other hand, at alkaline pH the enzyme is active toward *p*-nitrophenyl phosphate in the presence of magnesium ions (optimal pH 8–8.5), but not in the presence of zinc ions [3]. Moreover, at acidic pH the Zn-activated enzyme is able to hydrolyze L-phosphotyrosine with twice the affinity as for *p*-nitrophenyl phosphate, although with a lower V_{max}.

Myo-inositol-1-phosphatase is a key enzyme in receptor-stimulated phospholipid metabolism, and has been considered to be the target of Li^{+} ions in the treatment of manic depressive disease [4,5]. The fact that the enzyme is highly active toward *p*-nitrophenyl phosphate (an analog of phosphotyrosine) in the presence of Zn^{2+} ions at acidic pH suggests that *myo*-inositol-1-

☆ This study was supported by FIRB 2001 grants to G. Camici.
* Corresponding author. Dipartimento di Scienze Biochimiche, viale Pieraccini 6, I-50139 Firenze, Italy. Tel.: +39 55 4271394; fax: +39 55 4271394.
E-mail address: eugenio.giachetti@unifi.it (E. Giachetti).

0301-4622/$ - see front matter © 2006 Elsevier B.V. All rights reserved.
doi:10.1016/j.bpc.2006.10.004

phosphatase has undiscovered cellular functions, and may act as a phosphotyrosine protein phosphatase [3]. The brain contains vesicles that accumulate Zn^{2+} ions in millimolar concentrations (see Fraústo da Silva and Williams [6]). These authors suggest that these vesicles and the Zn^{2+} ion are involved in as yet undiscovered signalling processes. The phosphorylation of protein tyrosine is involved in several biological processes such as cell growth, differentiation, and transformation [7]. Phosphorylation of proteins on tyrosine is finely balanced by the activities of both phosphotyrosine protein phosphatases and phosphotyrosine protein kinases. The former enzymes are divided into membrane-bound and soluble subfamilies. Certain phosphotyrosine protein phosphatases, such as that from *Yersinia pestis*, are involved in the mechanism of bacterial pathogenesis [8], and others, such as the product of the cdc25 gene, are involved in control of the cell cycle [9]. All known phosphotyrosine protein phosphatases catalyze the hydrolysis of *p*-nitrophenyl phosphate, and use a common catalytic mechanism with no metal ions involved. The kinetic and catalytic mechanism of Mg-dependent inositol phosphatase has been widely investigated, but nothing is known about the kinetics of its Zn-dependent activity. In the present work, we studied the mechanism of the aryl-phosphatase activity of the enzyme that requires the Zn^{2+} ion to catalyze the reaction at acidic pH. The kinetic analysis requires the *p*-nitrophenyl phosphate basicity constants and the stability constant of the Zn·*p*-nitrophenyl phosphate complex, and the first part of this investigation is concerned with the measurement of these constants.

2. Experimental procedures

2.1. Potentiometric measurements of p-nitrophenyl phosphate

Potentiometric titrations were carried out at 25 °C in 0.1 M NaCl with a previously described apparatus [10]. A digital PHM-84 Radiometer potentiometer, equipped with a glass and a reference electrode (from Radiometer), was connected to a personal computer together with a Metrohm Multidosimat piston burette. Titration curves were automatically controlled by a specifically written program and the e.m.f. (mV) in relation to V_T (ml of sodium hydroxide titrant) stored for further processing. A thermostated glass cell was filled with ca. 100 ml of 0.1 M NaCl in which a weighted amount of ligand (*p*-nitrophenyl phosphate) and a known excess of standardized hydrochloric acid solution was dissolved by magnetic stirring. A presaturated nitrogen stream was maintained over the surface of the solution to avoid CO_2 contamination. The complex formation with zinc(II) was studied in a similar manner by stepwise addition of standard 0.1 M NaOH solution to an acidic solution containing a ligand/zinc(II) molar ratio of 1 and 2. Table 1 summarizes the experimental details of potentiometric titrations, with and without metal (II) ion. The basicity and stability constants were evaluated by the SUPERQUAD program [11].

2.2. Enzyme purification

The *myo*-inositol-1-phosphatase/aryl-phosphatase was prepared as described in Ref. [3].

Table 1
Experimental details of potentiometric measurements at 25 °C in 0.1 M NaCl

T_L (mmol)	$T_{Zn^{2+}}$ (mmol)	T_{H^+} (mmol)	C_T (mol dm^{-3})	pH-range	Points[a]
0.0819		0.3159	0.1023	2.70–4.32	55
0.0819	0.0426	0.3309	0.1023	3.30–6.24	35
0.1627		0.5292	0.0988	2.75–5.38	58
0.1627	0.1732	0.4330	0.0988	4.00–6.22	41

T_L: initial amount of ligand (*p*-nitrophenyl phosphate); T_{Zn2+}: initial amount of zinc(II) ions; T_{H^+}: initial amount of hydrogen ions; C_T: titrant sodium hydroxide standard solution.
[a] Number of points from titration curve.

2.3. Enzyme assay

Enzyme activity was determined using the general phosphatase substrate *p*-nitrophenyl phosphate in 0.1 M 2-(*N*-morpholino)ethanesulfonic acid-NaOH pH 5.5, containing suitable amounts of $ZnCl_2$ in a final volume of 1.0 ml, at 25 °C. The test was started by adding 100 μg of enzyme; the reaction was stopped after 1 min of incubation by adding 4 ml of 0.1 M KOH and the released *p*-nitrophenolate was measured at 400 nm ($\varepsilon = 18{,}000\ M^{-1}\ cm^{-1}$). We had previously established that the formation of *p*-nitrophenolate was linear at least up to 3 min of reaction time.

One unit of enzyme activity is defined as the amount of enzyme that catalyses the hydrolysis of 1 μmol of *p*-nitrophenyl phosphate per minute. Where appropriate, enzyme activity is reported as molar activity (mM s^{-1}). We used *p*-nitrophenyl phosphate obtained from Merck, because that available from other companies contained appreciable amounts of inorganic phosphate (about 1%), which is a competitive inhibitor of the enzyme (see below).

The model for zinc activation was determined from the kinetic analysis of a set of initial velocity measurements. Enzyme activity was assayed varying total *p*-nitrophenyl phosphate concentration (range 0.1–15 mM), at various fixed Zn^{2+} concentrations (range 0.25–20 mM). Total Zn^{2+} concentration was adjusted each time in order to keep free Zn^{2+} concentration constant within each series at fixed value, as required by the kinetic treatment applied [12].

Phosphate inhibition with respect to substrate was evaluated varying free *p*-$NPPH^-$ concentration (range 0.067–1.35 mM) at five different fixed concentrations of free Zn^{2+} (range 0.25–5.0 mM); phosphate inhibition with respect to Zn^{2+} was evaluated varying free Zn^{2+} concentration (range 0.25–5.0 mM) at five different fixed concentrations of free *p*$NPPH^-$ (range 0.067–1.35 mM). In both cases, five fixed total phosphate concentrations were used in the range 0–2 mM.

The effect of *p*-nitrophenol was studied by assaying the amount of phosphate released, using the method described in Ref. [3].

2.4. Nomenclature

The monoprotonated and the fully ionised forms of *p*-nitrophenyl phosphate (*p*$NPPH_2$) are denoted as *p*$NPPH^-$ and *p*NPP^{2-}, respectively. E represents free enzyme, S free substrate, Zn free Zn^{2+}, and ZnS the Zn·*p*-nitrophenyl phosphate complex (Zn·*p*$NPPH^+$).

In rapid-equilibrium systems, constants with a capital K are the dissociation constants of the enzyme-ligand(s) complexes; their meaning is defined each time. k_p is the rate of dissociation of the productive enzyme-substrate complex into free enzyme and products (P).

In steady-state systems, the meaning of the kinetic constants is defined each time; k_i are the rate constants of the i-th single steps. The minus sign denotes the reverse step.

2.5. Calculations

The concentrations of free pNPPH$^-$, free pNPP^{2-}, free metal ion, and metal ion-p-nitrophenyl phosphate complex were calculated from the expression of the stability constant (K_{ass}) of the Zn·p-nitrophenyl phosphate complex:

$$K_{ass} = \frac{[\text{Zn}\cdot p\text{NPPH}^+]}{[p\text{NPPH}^-]\cdot[\text{Zn}^{2+}]} \quad (1)$$

which after substituting for:

$$[\text{Zn}\ p\text{NPPH}^+] = [p\text{NPPH}_{2t}] - ([p\text{NPPH}^-] + [p\text{NPP}^{2-}])$$

$$[\text{Zn}^{2+}] = [\text{Zn}_t^{2+}] - [\text{Zn}\ p\text{NPPH}^+]$$

becomes:

$$K_{ass} = \frac{[p\text{NPPH}_{2t}] - [p\text{NPPH}^-] - [p\text{NPP}^{2-}]}{[p\text{NPPH}^-]\cdot([\text{Zn}_t^{2+}] - [p\text{NPPH}_{2t}] + [p\text{NPPH}^-] + [p\text{NPP}^{2-}])} \quad (2)$$

where $[p\text{NPPH}_{2t}]$=total p-nitrophenyl phosphate concentration, $[\text{Zn}_t^{2+}]$=total Zn^{2+}concentration, and $[p\text{NPP}^{2-}] = \frac{K_a''}{[\text{H}^+]}\cdot p\text{NPPH}^-]$, with K_a'' second dissociation constant of p-nitrophenyl phosphate.

Free pNPPH$^-$ concentration was the positive root of the resulting quadratic equation:

$$K_{ass}\left(1 + \frac{K_a''}{[\text{H}^+]}\right)\cdot[p\text{NPPH}^-]^2 + \left(1 + \frac{K_a''}{[\text{H}^+]} + K_{ass}[\text{Zn}_t^{2+}] - K_{ass}[p\text{NPPH}_{2t}]\right) \times [p\text{NPPH}^-] - [p\text{NPPH}_{2t}] = 0$$

where K_{ass}=240 M^{-1}, $K_a''=8.32\times10^{-6}$ M (see below), and $[\text{H}^+]=3.16\times10^{-6}$ M, being pH=5.5. The other forms were readily determined from the relationships given above.

2.6. Discrimination of the kinetic models

Starting from simple reaction mechanisms, we introduced additional equilibria, step by step up to include all the possible enzyme species present in our system. The corresponding velocity equations were derived assuming rapid-equilibrium conditions. The kinetic parameters in these equations were determined by nonlinear regression (based on least-square fitting), using the program Systat 5.1 running on an iMac (Apple Computer). The program implements two different algorithms (Quasi-Newton and Simplex) to find the parameter values that minimize the sum-of-squares-of-residuals (SSR); i.e. satisfying the equation:

$$\sum_{i,j}(v_{ij}\text{theo} - v_{ij}\text{obs})^2 = \text{minimum}$$

where v_{ij}theo are the expected rates at any i-th substrate and j-th ion concentrations, and v_{ij}obs are the corresponding experimental rates.

The wide range of substrate and Zn^{2+}concentrations used should be sufficient to ensure experimental conditions allowing the discrimination of the proper model.

The superiority between rival models, or the significance of the improvement obtained by introducing an additional parameter in a simpler mechanism, were tested by two-tailed F-statistic on empirical variances. Empirical variance is defined as the ratio SSR over $n-p$, with n number of observations, and p number of parameters contained in the model. P (significance level) is the probability of the equality of variances being due to chance alone. Any further improvement of a model was rejected in the case that its significance level was not at least less than 0.1. In addition, models failing to converge during the minimization procedure or yielding unreasonable parameter values were considered inferior [13], and therefore discarded.

The experimental variance was calculated from replicate measurements of initial velocity at different substrate and ion concentrations. The standard deviation values suggested that the relative error is almost constant. However, no weighting factor was applied in regression analysis.

Table 2
Basicity and stability constants at 25 °C in 0.1 M NaCl

Reaction	log$K$	logβ
pNPP^{2-}+H$^+$=pNPPH$^-$	5.0792 (9)	
pNPPH$^-$+H$^+$=pNPPH$_2$	1.501 (11)	
pNPP^{2-}+Zn^{2+}+H$^+$=Zn·pNPPH$^+$		7.46 (5)
pNPPH$^-$+Zn^{2+}=Zn·pNPPH$^+$		2.38 (5)
pNPP^{2-}+Zn^{2+}+2OH$^-$=Zn(OH)$_2$·pNPP^{2-}		15.53 (2)

pNPP^{2-} and pNPPH$^-$ indicate the fully ionised and the monoprotonated forms of p-nitrophenyl phosphate (pNPPH$_2$), respectively. Zn·pNPPH$^+$ indicates the Zn·p-nitrophenyl phosphate complex.
The figures between brackets is an estimate for the error in the last significant digit.

3. Results

3.1. Basicity and stability constants

Table 2 reports the basicity and stability constants with zinc (II) ions, evaluated as described under Experimental Procedures.

The p-nitrophenyl phosphate in the ionised form (pNPP^{2-}) showed two log$K$ values, the second one being less accurate because of the small amount of protonated species. However, the logK_1 is in line with the values reported in the literature [14].

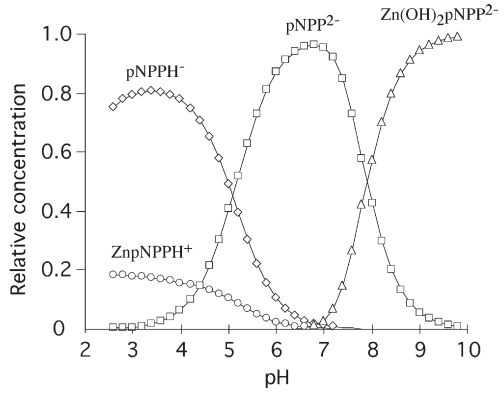

Fig. 1. Relative distribution of *p*-nitrophenyl phosphate forms as a function of pH, in the presence of equimolar concentrations of total *p*-nitrophenyl phosphate and Zn^{2+}. (◇) *p*NPPH$^-$, (□) *p*NPP^{2-}, (○) Zn·*p*NPPH$^+$, (△) Zn(OH)$_2$*p*NPP^{2-}.

The zinc(II)-*p*-nitrophenyl phosphate complex system was studied with two different ligand/metal-ion molar ratios. Among the different stoichiometries tested, the program Superquad [11] refined only two complex species, in two different ranges of pH. The former species, of Zn·*p*NPPH$^+$ stoichiometry, formed appreciably in the low range of pH (3.30–6.24) and involves an electrostatic bond between Zn^{2+} and the negatively charged ligand in the monoprotonated form (*p*NPPH$^-$). This species is consistent with the low stability constant (logβ=2.38). The latter species is a hydroxo-complex of Zn(OH)$_2$*p*NPP^{2-} stoichiometry that formed appreciably at pH higher than 7. The presence of this species is usually found in many systems of polymeric nature [15] and displays high logβ values. Fig. 1 shows the relative distribution of the *p*-nitrophenyl phosphate forms in the pH range 2–10.

3.2. Rapid-equilibrium mechanism

Fig. 2a, b show the substrate saturation curves at various fixed concentrations of free Zn^{2+}. As the Zn^{2+} concentration increases, the substrate saturation curves deviate more and more from hyperbolic behavior, and are affected by apparent substrate inhibition, which becomes obvious at high Zn^{2+} concentrations.

We found that this effect was not due to free *p*NPPH$^-$ and/or free Zn^{2+}, as may be the case for some metal-ion-activated enzymes [16]. Consequently, the usual methods for determining the activation mechanism (see for example the criteria proposed by London and Steck [17]) are useless in our situation. Because of this inhibition, there is no simple way to evaluate the apparent kinetic parameters, as suggested in Refs. [12,18]. In short, the choice of appropriate activation mechanism is based on statistical comparison of possible models, evaluating their least-squares fit to the experimental data.

We found that zinc ions are definitely needed for the aryl-phosphatase activity of *myo*-inositol-1-phosphatase [3]. It follows that the catalytically productive enzyme species must be at least a ternary EZnS complex, independently of its co-ordination structure and apart from the pathways leading to its formation, which can be many and kinetically indistinguishable as, for example, in the reactions:

$$E \overset{Zn}{\rightleftarrows} E \cdot Zn \overset{S}{\rightleftarrows} E \cdot Zn \cdot S$$

or

$$E \overset{ZnS}{\rightleftarrows} E \cdot ZnS$$

The possible activation mechanisms can be grouped into two categories: (i) essential activation and (ii) in which a metal-substrate complex is the true substrate. The term "essential activator" is used in the strict sense of the word: the ion binds to a specific activation site and S or ZnS can only bind to the activated enzyme form (Zn·E); only Zn·E·S and/or Zn·E·ZnS are catalytically active [18].

3.2.1. Essential activation

Preliminary screening of the experimental data suggested that the simplest mechanism, which also accounts for the observed inhibition, is described by model I assuming essential

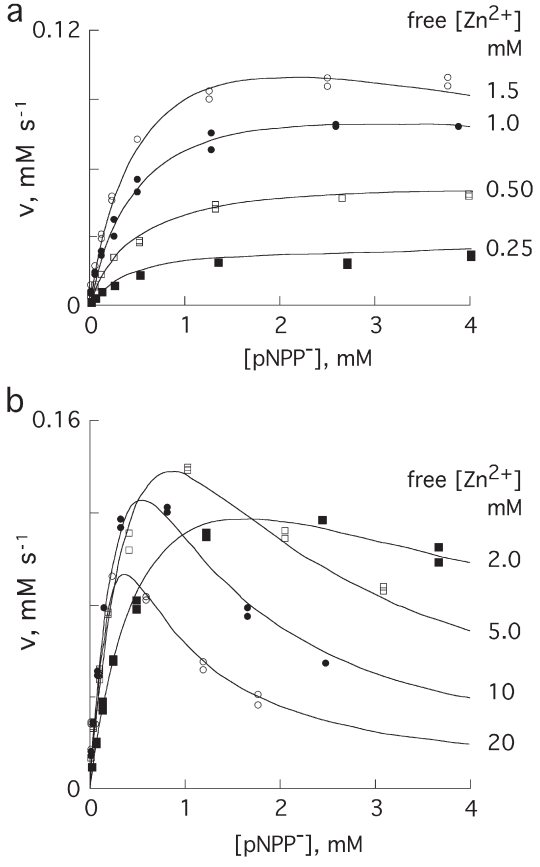

Fig. 2. Substrate saturation curves at different fixed concentrations of free Zn^{2+}. In a: (■) 0.25 mM, (□) 0.5 mM, (●) 1.0 mM, (○) 1.5 mM; in b: (■) 2.0 mM, (□) 5.0 mM, (●) 10 mM, (○) 20 mM. Curves were drawn according to the best-estimated mechanism for Zn-activation (mechanism XV), substituting the values reported in Table 4 for the parameters in Eq. (6).

Table 3
Enzyme species involved in the models fitted to the experimental data

Model	Enzyme species							Variance
I	E	Zn·E			Zn·E·ZnS*		Zn·E·ZnS·ZnS	0.893
II[a]	E	Zn·E	Zn·E·Zn		Zn·E·ZnS*		Zn·E·ZnS·ZnS	0.430
III[b]	E	Zn·E		Zn·E·S	Zn·E·ZnS*		Zn·E·ZnS·ZnS	0.848
IV	E	Zn·E	Zn·E·Zn	Zn·E·S	Zn·E·ZnS*		Zn·E·ZnS·ZnS	0.121
V[a]	E	Zn·E	Zn·E·Zn	E·Zn	Zn·E·ZnS*		Zn·E·ZnS·ZnS	0.433
VI[b]	E	Zn·E	Zn·E·Zn	E·S	Zn·E·ZnS*		Zn·E·ZnS·ZnS	0.207
VII	E	Zn·E	Zn·E·Zn	E·ZnS	Zn·E·ZnS*		Zn·E·ZnS·ZnS	0.121
VIII	E	Zn·E	Zn·E·Zn	E·S	Zn·E·ZnS*	Zn·E·S	Zn·E·ZnS·ZnS	0.120
IX	E	Zn·E	Zn·E·Zn	Zn·E·S	Zn·E·ZnS*	Zn·E·Zn·ZnS	Zn·E·ZnS·ZnS	0.103
X	E				E·ZnS*		E·ZnS·ZnS	1.029
XI	E	E·Zn			E·ZnS*		E·ZnS·ZnS	0.981
XII	E		E·S		E·ZnS*		E·ZnS·ZnS	0.841
XIII	E	E·Zn	E·S		E·ZnS*		E·ZnS·ZnS	0.125
XIV[c]	E	E·Zn	E·S	E·S·ZnS	E·ZnS*		E·ZnS·ZnS	0.126
XV	E	E·Zn	E·S		E·ZnS*	E·Zn·ZnS	E·ZnS·ZnS	0.103
XVI[d]	E	E·Zn	E·S	E·Zn·Zn	E·ZnS*		E·ZnS·ZnS	0.114
XVII[e]	E	E·Zn	E·S	E·S·S	E·ZnS*		E·ZnS·ZnS	0.126
XVIII[d]	E	E·Zn	E·S	E·Zn·Zn	E·ZnS*	E·Zn·ZnS	E·ZnS·ZnS	0.101
XIX[e]	E	E·Zn	E·S	E·S·S	E·ZnS*	E·Zn·ZnS	E·ZnS·ZnS	0.104
XX[c]	E	E·Zn	E·S	E·S·ZnS	E·ZnS*	E·Zn·ZnS	E·ZnS·ZnS	0.104

An asterisk indicates the productive enzyme species.
E, free enzyme; Zn, Zn^{2+} ion; S, monoprotonated *p*-nitrophenylphosphate; ZnS, Zn·*p*NPPH$^+$ complex.
Model IV and VII are homomorphous given that Zn·E·S and E·ZnS imply the same mathematical expressions.
While the separate introduction of the E·Zn and E·S species in model X does not produce substantial improvements, their simultaneous addition (model XIII) cuts down the variance drastically. The same observation applies to models I–IV.
[a] Convergence to minimum with the value of K_{EA} (dissociation constant of the Zn·E complex)→∞.
[b] Convergence to minimum with a negative value of K_{EA}.
[c] Convergence to minimum with the constant for dissociation of E·S·ZnS to E·S+ZnS→∞.
[d] Fitting of these models yields high values of the constant for the dissociation of E·Zn·Zn to E·Zn+Zn.
[e] Convergence to minimum with the constant for dissociation of E·S·S to E·S+S→∞.

activation, or model X in the case that Zn-substrate complex is the true substrate.

Model I is represented by the following reaction scheme:

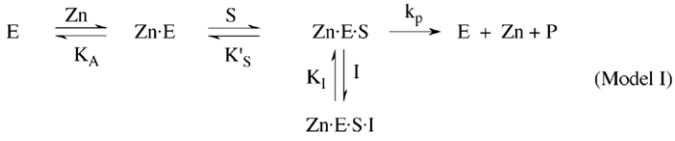

(Model I)

Where S can be either *p*NPPH$^-$, *p*NPP^{2-}, or Zn·*p*NPPH$^+$and I indicates an unspecified ligand (Zn^{2+}, *p*NPPH$^-$, Zn·*p*NPPH$^+$, etc.) which is responsible of the apparent substrate inhibition.

The corresponding velocity equation, derived according to Rapid-Equilibrium assumptions, is:

$$v = \frac{V_{max}\frac{[Zn][S]}{K_A K'_S}}{1 + \frac{[Zn]}{K_A} + \frac{[Zn][S]}{K_A K'_S} \cdot \left(1 + \frac{[I]}{K_I}\right)} \quad (3)$$

As shown in Table 3, the best fit of this equation to the experimental data is obtained when both S and I are Zn·*p*NPPH$^+$. The factor $(1+I/K_I)$ must multiply one denominator term containing the substrate concentration in order to provide a second-degree equation which accounts for substrate inhibition; moreover, the enzyme species which binds I produces a "dead-end" complex.

Introduction of additional equilibria into model I yields the results listed in Table 3, where each model is denoted by the enzyme species involved in it. Of the mechanisms implying essential activation (I–IX), the simplest one providing the best fit (least variance) is model IV. Model VII, which gives the same variance as model IV, is homomorphous with this; in fact, the enzyme species Zn·E·S and E·ZnS, which make the difference between them, are the same form, being kinetically indistinguishable.

The improvement obtained by introducing the Zn·E·Zn·ZnS species in model IV (model IX) is not statistically significant according to the *F*-test ($P=0.37$). However, since the variance for model IX does not differ significantly from the experimental variance (0.082, $n=56$), unlike that for model IV, we consider model IX statistically superior to model IV.

3.2.2. Metal-substrate complex is the true substrate

In this case, the simplest model is the following:

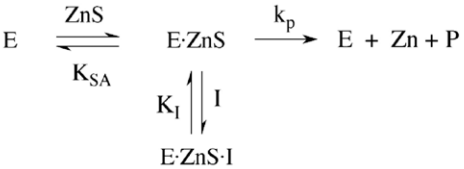

(Model X)

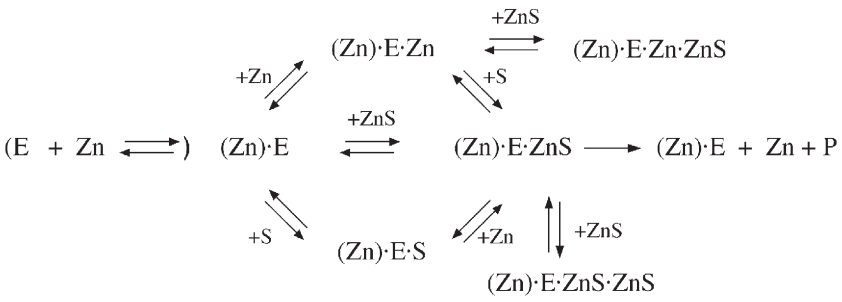

Fig. 3. Rapid-Equilibrium mechanism for zinc-ion activation of *myo*-inositol-1-phosphatase. The reaction between brackets is distinctive of model IX (which describes essential activation) and indicates the binding of the zinc ion to an activation site. E, free enzyme; S, *p*NPPH$^-$ (or *p*NPP^{2-}); ZnS, Zn·*p*NPPH$^+$; P, products; (Zn)·S, metal activated enzyme.

Where ZnS is the Zn·*p*NPPH$^+$ complex, and I has the same meaning as in model I. The corresponding velocity equation is:

$$v = \frac{V_{max}\frac{[ZnS]}{K_{SA}}}{1+\frac{[ZnS]}{K_{SA}}\cdot\left(1+\frac{[I]}{K_I}\right)} \quad (4)$$

As in the case for essential activation, Eq. (4) yields the best fit when I=Zn·*p*NPPH$^+$ (see Table 3).

The results of regression analysis upon introducing additional equilibria are shown in Table 3 (models X–XX). Models within this group follow the same patterns as those previously mentioned. In particular, the remarks concerning models IV (or VII) and IX also apply to models XIII and XV, with the latter mechanism statistically superior to model XIII.

In addition to the catalytically active E·ZnS complex, model XV implies the existence of both a E·Zn and a E·S species, suggesting that the E·ZnS form can originate from five distinct steps, involving free Zn^{2+}, free S and the ZnS complex.

Models IX and XV may therefore both be depicted by a rapid-equilibrium random mechanism with two dead-end

Table 4
Parameter values obtained by fitting Eq. (5) (model IX) and Eq. (6) (model XV) to the experimental data

	Model IX (essential activation)	Model XV (ZnS substrate)
	mM s^{-1} (±S.E.)	mM s^{-1} (±S.E.)
V_{max}	0.70±0.15	0.67±0.13
	mM (±S.E.)	mM (±S.E.)
K_{EA}	0.10±0.10	–
K_A	3.8±0.6	4,0±0.6
K_S	0.48±0.06	0.51±0.06
K_S'	0.69±0.07	0.67±0.06
K_{AS}	2.1±0.6	1.9±0.6
K_I	0.80±0.04	0.80±0.04
Variance	(mM s^{-1})^2	(mM s^{-1})^2
	2.85×10^{-5}	2.86×10^{-5}

Model IX (Eqn. 5):

$K_{EA} = [E]\cdot[Zn]/[Zn\ E]$,
$K_A = [Zn\ E]\cdot[Zn]/[Zn\ E\ Zn]$,
$K_S = [Zn\ E]\cdot[S]/[Zn\ E\ S]$,
$K_S' = [Zn\ E\ Zn]\cdot[S]/[Zn\ E\ Zn\ S]$,
$K_{AS} = [Zn\ E\ Zn]\cdot[(ZnS)]/[Zn\ E\ Zn(ZnS)]$,
$K_I = [Zn\ E\ ZnS]\cdot[(ZnS)]/[Zn\ E\ Zn\ S(ZnS)]$.

Model XV (Eqn. 6):

$K_A = [E]\cdot[Zn]/[E\ Zn]$,
$K_S = [E]\cdot[S]/[E\ S]$,
$K_S' = [E\ Zn]\cdot[S]/[E\ Zn\ S]$,
$K_{AS} = [E\ Zn]\cdot[(ZnS)]/[E\ Zn\ (ZnS)]$,
$K_I = [E\ Zn\ S]\cdot[(ZnS)]/[E\ Zn\ S\ (ZnS)]$.

In both models: S, monoprotonated *p*-nitrophenylphosphate; (ZnS), Zn·*p*NPPH$^+$ complex.

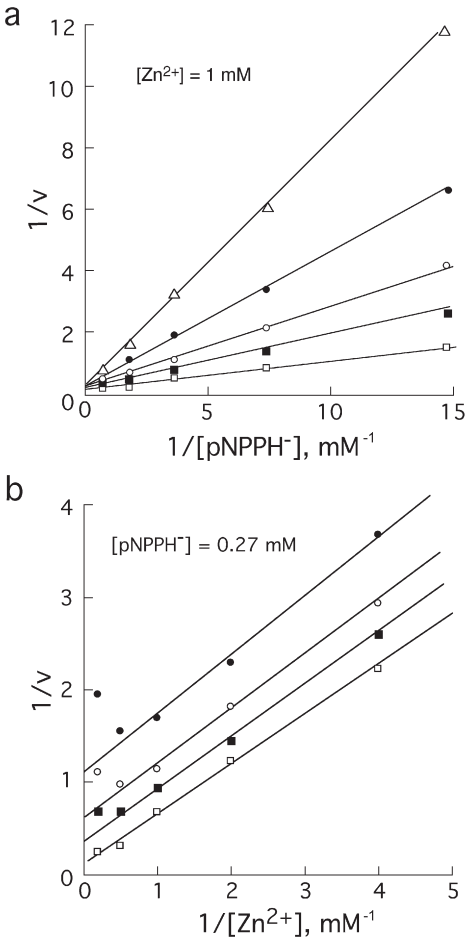

Fig. 4. Double reciprocal plots of $1/v$ vs. $1/[p\text{NPPH}^-]$ (a), and $1/v$ vs. $1/[Zn^{2+}]$ (b) at various fixed concentrations of phosphate (□ no phosphate, ■ 0.25 mM, ○ 0.5 mM, ● 1.0 mM, △ 2 mM). *v* indicates initial velocity (arbitrary units). In b, the experimental data deviate from linearity at high $[Zn^{2+}]$, due to the strong Zn·*p*NPPH$^+$ inhibition, that is even more marked owing to the presence of added phosphate.

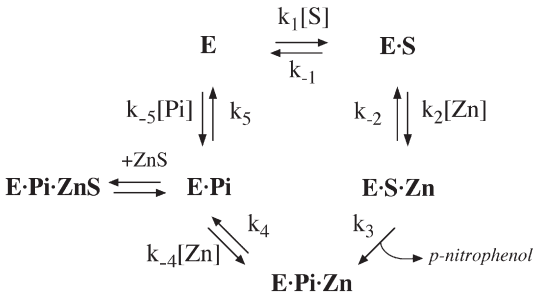

Fig. 5. Kinetic mechanism of *myo*-inositol-1-phosphatese under steady-state conditions. Pi indicates inorganic phosphate; S, *p*NPPH$^-$; ZnS, Zn·*p*NPPH$^+$.

inhibition steps caused by the metal-substrate complex, as shown in Fig. 3.

The complete velocity equations are given below. Eq. (5) refers to the case of essential activation, and Eq. (6) to the case in which the Zn-*p*NPPH$^+$ complex is the substrate of the reaction.

$$v = \frac{V_{\max}\frac{[Zn][Zn][S]}{K_{EA}K_AK'_S}}{1+\frac{[Zn]}{K_{EA}}+\frac{[Zn][Zn]}{K_{EA}K_A}+\frac{[Zn][S]}{K_{EA}K_S}+\frac{[Zn][Zn][ZnS]}{K_{EA}K_AK_{AS}}+\frac{[Zn][Zn][S]}{K_{EA}K_AK'_S}\cdot\left(1+\frac{[ZnS]}{K_I}\right)} \quad (5)$$

$$v = \frac{V_{\max}\frac{[Zn][S]}{K_AK'_S}}{1+\frac{[Zn]}{K_A}+\frac{[S]}{K_S}+\frac{[Zn][ZnS]}{K_AK_{AS}}+\frac{[Zn][S]}{K_AK'_S}\cdot\left(1+\frac{[ZnS]}{K_I}\right)} \quad (6)$$

Although model XV assumes Zn*p*NPPH$^+$ complex to be the substrate of the reaction, Eq. (6) is given in terms of free Zn^{2+} and free S for a more direct comparison with Eq. (7).

The values of the kinetic parameters for these two alternative models, obtained from fitting the corresponding equations to the experimental data, are shown in Table 4.

As is evident from the scheme in Fig. 3, as well as from the enzyme species involved in these mechanisms, models IX and XV differ each from each other solely in the binding of one zinc ion to an enzyme activation site. They yield identical variances (Table 4) as a result of the equally good fit of Eqs. (5) and (6) to the experimental data. Moreover, K_{EA}, the constant that refers to the essential activation, is a redundant parameter, as shown by the high standard error on its estimate (Table 4). In short, model IX is effectively an extension of model XV that does not introduce significant improvements. This also means that the binding of Zn ion to an enzyme activation site is not kinetically important, even if it is required catalytically.

In conclusion, we retain model XV, the simpler one, as the best mechanism describing Zn activation of the intrinsic aryl-phosphatase activity of *myo*-inositol-1-phosphatase.

3.3. Steady-state kinetic mechanism

In addition to describing a Rapid-Equilibrium random mechanism, Eq. (6) (or (5)) is consistent with a sequentially ordered mechanism under steady-state conditions. The binding order of substrate and ion cannot be directly deduced from this equation. However, it is very likely that zinc binds after the substrate, as suggested by the existence of the E·Zn·Zn·S species which indicates that a metal ion dissociates from the ternary complex before the release of the last product. In other words, there would not be an E·Zn species under steady-state assumptions.

This hypothesis is supported by the type of phosphate inhibition, which is competitive with respect to substrate but uncompetitive with respect to Zn^{2+}, as shown in Fig. 4a, b.

To recapitulate, assuming steady-state conditions, Zn-dependent activity of *myo*-inositol-1-phosphatase obeys a sequentially ordered mechanism, with substrate binding before the metal ion, as shown in Fig. 5.

The central complex (E·S·Zn) breaks down irreversibly, liberating *p*-nitrophenol and leaving a E·Pi·Zn form. The catalytic cycle ends with two reversible steps, during which the zinc ion and inorganic phosphate are released from the enzyme in that order. The lack of any effect by *p*-nitrophenol also confirms the overall mechanism.

The initial velocity equation (Pi=0) for this mechanism is the following:

$$v = \frac{V_{\max}[S][Zn]}{K_sK'_s+K_a[Zn]+K'_s[S]+K_{as}[S][Zn][Zn]+K_{sa}[S][Zn]\cdot\left(1+\frac{[ZnS]}{K_I}\right)} \quad (7)$$

This is a rearrangement of Eq. (6) to a form more appropriate for a steady-state system; the meaning and values of the kinetic constants are given in Table 5.

Table 5
Kinetic and rate constants for the steady-state mechanism of inositol-phosphatase

$V_{\max}=k_3[E_t]=1.1$ mM s^{-1}	$K_s=\frac{k_{-1}}{k_1}=0.60$ mM	$K'_s=\frac{k_{-2}+k_3}{k_2}=4.8$ mM
$K_a=\frac{k_3}{k_1}=0.62$ mM	$K_{as}=\frac{k_3}{k_5}\cdot\frac{k_{-4}}{k_4}=0.09$ mM	$K_{sa}=\frac{k_3k_4+k_3k_5+k_4k_5}{k_4k_5}=1.1$
$K_p=\frac{k_{-5}}{k_5}=1.2$ mM	$K_{ap}=\frac{k_{-4}}{k_4}=4.6$ mM	K_I=dissociation constant of the E·Pi·ZnS complex=0.80 mM

k_1	k_{-1}	k_3	k_4	k_{-4}	k_5	k_{-5}
650 mM^{-1} s^{-1}	390 s^{-1}	400 s^{-1}	9.2×10^5 s^{-1}	4.2×10^6 mM^{-1} s^{-1}	2.0×10^4 s^{-1}	2.4×10^4 mM^{-1} s^{-1}

The denominator term Zn·Zn·S, which results in the Rapid-Equilibrium mechanism from the dead-end reaction E·Zn + ZnS ⇄ E·Zn·ZnS (see Fig. 3), in the steady state system originates from the expression of the relative concentration of the E·Pi·Zn species (that is = $k_1k_2k_3k_5$[S][Zn] + $k_1k_2k_3k_{-4}$[Zn][Zn][S]). Moreover, substrate inhibition can here be ascribed to the binding of the ZnS complex with the E·Pi form, to give the dead-end E·Pi·ZnS species. This binding seems more probable than binding of the same ion-substrate complex with the E·Zn·S species, as the rapid-equilibrium model implies.

The complete velocity equation, which also accounts for phosphate inhibition, contains three additional denominator terms: $K_sK'_sK_p$[Pi] + ($K_sK'_sK_pK_{ap} + K_aK_p$)[Pi][Zn] + $K_aK_pK_{ap}$[Pi][Zn][Zn]. The values of K_p and K_{ap} permit calculation of the full set of rate constants, except k_2 and k_{-2} which remain undetermined (see Table 5). It is, however, possible to estimate that, as the Zn^{2+} concentration remains below 3 mM, more than 90% of the total enzyme is distributed between free enzyme and the enzyme-substrate complex (the proportions depend on the substrate concentration), so that the rate limiting steps of the overall reaction is probably controlled by the availability of zinc ions. The exclusive role of zinc ions in the activity of brain *myo*-inositol phosphatase at acidic pH is also corroborated by the following observations: that no enzyme activity is detected in the absence of this ion, that Mg cannot replace Zn [3], and that Mg (at least up to 5 mM) has no inhibitory effect with respect to either saturating or unsaturating Zn concentrations.

4. Discussion

Several studies [19–22] indicate that the kinetic mechanism of the Mg-dependent inositol phosphatase follows a sequentially ordered mechanism, in which inositol-1-phosphate binds to the Mg-activated enzyme prior to the binding of a second Mg ion. This metal ion allows a nucleophilic water molecule to break down the substrate phosphoester bond, following which inositol debinds to leave phosphate ligated to both Mg ions. The free enzyme is subsequently regenerated by the release of Mg^{2+} and phosphate, in that order.

The present paper has shown that the Zn-dependent aryl-phosphatase activity of the enzyme follows the same steady-state ordered mechanism, with some minor differences.

As in the study by Leech et al. [19], we found no evidence for the participation, in the kinetic mechanism, of an ion previously bound to the enzyme metal-site. Indeed, this ion was identified by means of structural studies [21,23,24], and this finding led Pollack and co-workers to suggest a three-metal assisted catalytic mechanism. We have already stated that an additional activating zinc ion may be required catalytically, although it is kinetically irrelevant in our experimental model. The metal-site affinity for that ion is probably so high that the minimal enzyme species we deal with in our mechanism is a Zn-activated enzyme.

Leech et al. [19] also observed a cooperative effect for Mg^{2+} binding with inositol-1-phosphate as the substrate, but not with inositol-4-phosphate. In our kinetic analysis we found no cooperativity for Zn^{2+} binding.

Another difference is the pathway leading to Zn-*p*NPPH$^+$ inhibition, as a consequence of its binding to the enzyme-phosphate species (E·Pi in Fig. 5). The existence of this equilibrium was not detected in the kinetic [21] and structural [22–24] studies on the Mg-dependent inositol phosphatase. A possible reason is the lack of a monopositive Mg-inositol phosphate complex at neutral pH. However, these authors ascribed the observed lithium inhibition to the binding of Li^+ ion to the enzyme-phosphate species remaining after inositol is released. The inhibition by the monopositive Zn-*p*NPPH$^+$ complex in our model appears to mimic the effect of lithium [25], being directed toward the same enzyme species with similar result. The inhibitory effect of the zinc-substrate complex may be useful in regulating the Zn-dependent tyrosine phosphate activity of brain inositol-phosphatase in vivo [26]. In regard to the hypothesis that Zn-rich vesicles in the brain are involved in signalling processes [6], it may be significant that the enzyme is not active in the absence of Zn ions [3], and that Mg has no competitive effect on the Zn-dependent activity of inositol phosphatase at acidic pH.

Acknowledgments

We are profoundly grateful to Professor Giampietro Ramponi for his continuing interest in our work and his qualified suggestions.

References

[1] S. Fujimoto, H. Gotoh, T. Ohbayashi, H. Yazaki, A. Ohara, Purification and characterization of zinc-dependent acid phosphatase from bovine brain, Biol. Pharm. Bull. 16 (1993) 745–750.
[2] F. Panara, The presence of a Zn^{2+}-dependent acid *p*-nitrophenyl phosphatase in bovine liver. Isolation and some properties, Biochem. J. 235 (1986) 265–268.
[3] A. Caselli, P. Cirri, S. Bonifacio, G. Manao, G. Camici, G. Cappugi, G. Moneti, G. Ramponi, Identity of zinc ion-dependent acid phosphatase from bovine brain and *myo*-inositol 1-phosphatase, Biochim. Biophys. Acta 1290 (1996) 241–249.
[4] L.M. Hallcher, W.R. Sherman, The effects of lithium ion and other agents on the activity of *myo*-inositol-1-phosphatase from bovine brain, J. Biol. Chem. 255 (1980) 10897–10901.
[5] W.R. Sherman, A.L. Leavitt, M.P. Honcher, L.M. Hallcher, B.E. Phillips, Evidence that lithium alters phosphoinositide metabolism: chronic administration elevates primarily D-*myo*-inositol-1-phosphate in cerebral cortex of the rat, J. Neurochem. 36 (1981) 1947–1951.
[6] J.J.R. Fraústo da Silva, R.J.P. Williams, in: J.J.R. Fraústo da Silva, R.J.P. Williams (Eds.), The Biological Chemistry of the Elements, Clarendon Press, Oxford, 1991, p. 299.
[7] E.H. Fischer, H. Charbonneau, N.K. Tonks, Protein tyrosine phosphatases: a diverse family of intracellular and transmembrane enzymes, Science 253 (1991) 401–406.
[8] J.B. Bliska, K.L. Guan, J.E. Dixon, S. Falkow, Tyrosine phosphate hydrolysis of host proteins by an essential Yersinia virulence determinant, Proc. Natl. Acad. Sci. U. S. A. 88 (1991) 1187–1191.
[9] P. Nurse, Universal control mechanism regulating onset of M-phase, Nature 344 (1990) 503–508.
[10] M. Casolaro, Vinyl polymers containing L-valine and L-leucine residues: thermodynamic behavior of homopolymers and copolymers with *N*-Isopropylacrylamide, Macromolecules 28 (1995) 2351.
[11] P. Gans, A. Sabatini, A. Vacca, SUPERQUAD: an improved general program for computation of formation constants from potentiometric data, J. Chem. Soc., Dalton Trans. (1985) 1195–1200.

[12] E. Giachetti, P. Vanni, Effect of Mg^{2+} and Mn^{2+} on isocitrate lyase, a non-essentially metal-ion-activated enzyme. A graphical approach for the discrimination of the model for activation, Biochem. J. 276 (1991) 223–230.
[13] B. Mannervik, in: L. Endrenyi (Ed.), Kinetic Data Analysis, Design and Analysis of Enzyme and Pharmacokinetic Experiments, Plenum Press, New York, 1981, p. 235.
[14] N. Bourne, A. Williams, Effective charge on oxygen in phosphoryl (-PO32-) group transfer from an oxygen donor, J. Org. Chem. 49 (1984) 1200–1204.
[15] R. Barbucci, M. Casolaro, A. Magnani, Ionic and ionizable synthetic polymers: interactions in aqueous solutions, Coord. Chem. Rev. 120 (1992) 29–50.
[16] I.H. Segel, Enzyme Kinetics, Wiley, New York, 1975, p. 227.
[17] W.P. London, T.L. Steck, Kinetics of enzyme reactions with interaction between a substrate and a (metal) modifier, Biochemistry 8 (1969) 1767–1779.
[18] E. Giachetti, G. Pinzauti, R. Bonaccorsi, P. Vanni, Isocitrate lyase from *Pinus pinea*. Characterization of its true substrate and the action of magnesium ions, Eur. J. Biochem. 172 (1988) 85–91.
[19] A.P. Leech, G.R. Baker, J.K. Shute, M.A. Cohen, D. Gani, Chemical and kinetic mechanism of the inositol monophosphatase reaction and its inhibition by Li^{+}, Eur. J. Biochem. 212 (1993) 693–704.
[20] S.J. Pollack, H.B. Knowles, J.R. Atack, M.R. Broughton, C.I. Ragan, S. Osborne, G. McAllister, Probing the role of metal ions in the mechanism of inositol monophosphatase by site-directed mutagenesis, Eur. J. Biochem. 217 (1993) 281–287.
[21] S.J. Pollack, J.R. Atack, M.R. Knowles, G. McAllister, C.I. Ragan, R. Baker, S.R. Fletcher, L.L. Iversen, H.B. Broughton, Mechanism of inositol monophosphatase, the putative target of lithium therapy, Proc. Natl. Acad. Sci. U. S. A. 91 (1994) 5766–5770.
[22] J.R. Atack, H.B. Broughton, S.J. Pollack, Structure and mechanism of inositol monophosphatase, FEBS Lett. 361 (1995) 1–7.
[23] R. Bone, L. Frank, J.P. Springer, S.J. Pollack, S. Osborne, J.R. Atack, M.R. Knowles, G. McAllister, C.I. Ragan, H.B. Broughton, R. Baker, S.R. Fletcher, Structural analysis of inositol monophosphatase complexes with substrates, Biochemistry 33 (1994) 9460–9467.
[24] R. Gill, F. Mohammed, R. Badyal, L. Coates, P. Erskine, D. Thompson, J. Cooper, M. Gore, S. Wood, High-resolution structure of *myo*-inositol monophosphatase, the putative target of lithium therapy, Acta Crystallogr. 61 (2005) 545–555.
[25] J.R. Atack, H.B. Broughton, S.J. Pollack, Inositol monophosphatase—a putative target for Li^{+} in the treatment of bipolar disorder, Trends Neurosci. 18 (1995) 343–349.
[26] S. Fujimoto, J. Tsuda, N. Kawakami, H. Tanino, S. Shimohama, *Myo*-inositol monophosphatase in the brain has zinc ion-dependent tyrosine phosphatase activity, Gen. Pharmacol. 31 (1998) 469–475.